Transient simulation of a microburst outflow: Review and proposed new approach

William E. Lin, Cassie Novacco and Eric Savory

Department of Mechanical & Materials Engineering, University of Western Ontario, London, ON, N6A 5B9
Email: wlin25@uwo.ca, cnovacco@uwo.ca and esavory@eng.uwo.ca

The microburst is a wind event that can cause severe structural damage due to its intense, low-level outflow. Previous experiments have not created a sufficiently large flow to study the outflow wind load on urban structures. The present novel design simulates the key transient features and the test section flow can be made suitably large to accommodate further testing with aeroelastic models.

1. INTRODUCTION

Downbursts are strong vertical downdrafts that develop as part of the thunderstorm life cycle. As shown in Figure 1, they have sufficient energy to reach ground level. Impingement on the ground leads to a radially divergent outflow that bears strong resemblance to the wall jet discussed in the fluid mechanics literature.

Figure 1: *A downdraft column prior to impingement (Photo credit: Alan Moller ©).*

High-intensity downburst outflows tend to be less than 4 km in horizontal extent. These relatively small events are referred to as microbursts. In addition to the aviation incidents addressed in the early literature, microbursts also pose a hazard to urban structures because of the damaging wind speeds at the level of our built environment.

Fujita [1] describes an event with a 67 m/s peak gust speed recorded at 4.9 m above ground level. Such wind speeds are comparable to those in F2-F3 tornadoes. Figure 2 shows the catastrophic loss of a lattice tower in central Victoria, Australia in 1993. In Canada, tower failures have occurred in Manitoba. In particular, 17 structures failed during a September 1996 downburst event [2].

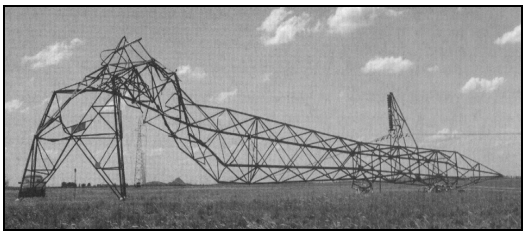

Figure 2: *Failure of a transmission line tower due to downburst wind loading [3].*

Furthermore, the microburst wind speed profile shape differs significantly from that of the conventional atmospheric boundary layer (ABL). For lattice tower design, in which specific members are designed for a specific loading mode, a difference in wind profile shape may be critical. Current structural design codes may not adequately account for microburst wind loads.

Previous experimental simulations have focused on the downdraft region, more so than the outflow region. With existing methods, the outflow region is not easily simulated on a physical scale that is amenable to wind load and aeroelastic testing of models. Thus, the present novel slot jet approach addresses the practical problem of maximizing the size of a laboratory flow that retains the key features of an intense microburst outflow.

2. KEY FLOW CHARACTERISTICS

As described by Fujita [1, 4], the downburst outflow has the following characteristics.

a) From the perspective of a stationary observer, a passing burst front is a transient phenomenon. As indicated in Figure 3, a ground anemometer records a clear velocity rise and fall as it encounters the burst front. Inset 1, which shows the anemometer just before the microburst reaches it, corresponds to the low ambient velocity in the time history. As the extreme wind region moves over the anemometer (Inset 2), the velocity time history rapidly attains a maximum.

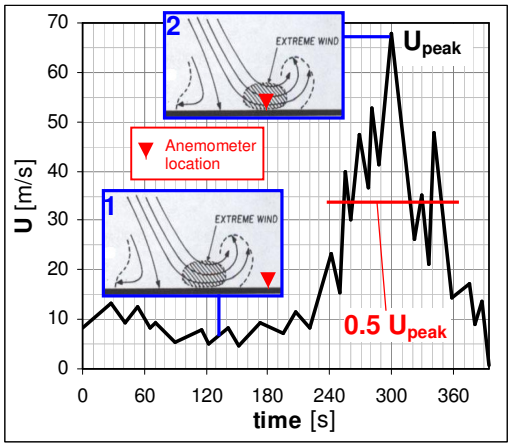

Figure 3: *Velocity time history from the Andrews AFB microburst. Adapted from [1].*

A rapid velocity reduction occurs after the maximum, because of the stagnation point in the eye of the microburst. The duration of $U > (0.5\ U_{peak})$ generally is less than 5 min. A weaker secondary peak may follow, as the other side of the microburst moves over the anemometer. The accompanying change in wind direction is dependent upon the translational path of the microburst. However, the critical loading is associated with the initial burst front, and the present work focuses on the primary velocity peak.

b) A vortex ring develops aloft about the downdraft column, reaches ground level, and expands outwards as the dominant feature of the outflow region. In Figure 4, downdraft impingement has occurred to the right and the development of the vortex ring is shown as it moves away from the impingement region.

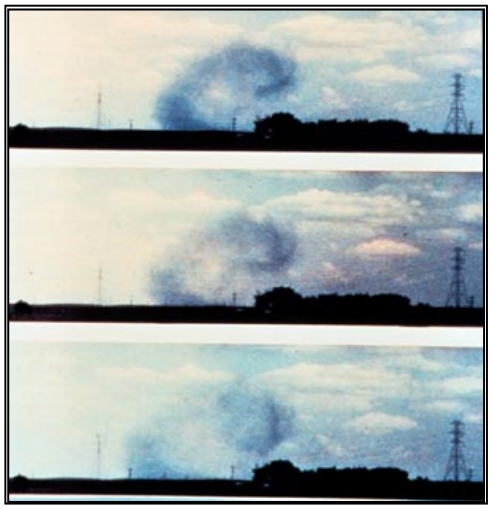

Figure 4: *An opportune series of photographs of the outflow region (Photo credit: Brian Waranauskas, NOAA Photo Library).*

Field observations are not extensive due to the relatively small size and brevity of the event. As a result, laboratory simulations are undertaken. Two methods have been employed in previous investigations.

2.1 Released fluid experiments

This experimental approach models the buoyancy-driven nature of the downburst. Figure 5 shows the typical apparatus. An outer tank (volume ~ 0.4 m^3) is filled with ambient fluid. A hollow cylinder (volume ~ 0.0003 m^3) is filled with fluid of greater density, and is mounted in the tank above a board upon which the dense fluid will impinge. A density differential ($\Delta\rho/\rho$) of 3-5% is typically chosen as representative of the negative buoyancy of a downburst.

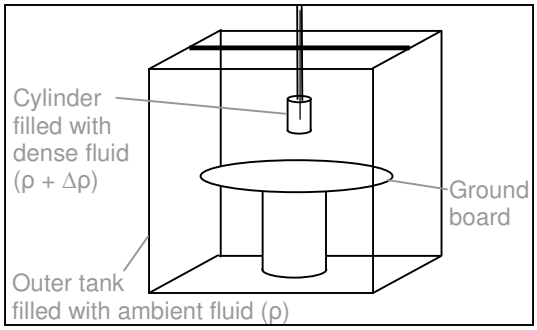

Figure 5: *Typical released fluid apparatus [5].*

Initially, the heavy fluid is retained in the cylinder with a thin rubber membrane over the lower end of the cylinder. Puncturing the

membrane with a needle impulsively starts the flow. The resulting impingement and outflow have been studied with flow visualization and Particle Image Velocimetry (PIV).

The vortex ring development has been studied extensively. After touchdown of the downdraft, Lundgren *et al* [6] found that the burst front accelerated to a maximum radial velocity and then decelerated to a nearly constant value. The radius of the equivalent spherical volume to the cylindrical release (R_0) was used in a dimensionless parameterization scheme.

PIV results by Alahyari & Longmire [7] show a sharp velocity gradient at the burst front. This suggests that an exposed structure experiences the microburst outflow as an abrupt load. The largest velocities occur at 0.05 R_0 above the surface.

Yao & Lundgren [8] show that the horizontal component of the outflow velocity is 4-6 times the vertical component. Near the peak velocity, fluctuations in the horizontal component can be 25-30% of the peak value due to interaction of the primary vortex with the ground, resulting in secondary vortices with opposing vorticity. The primary vortex ring is the dominant feature in the region of maximum intensity flow.

However, the peak of the vertical profile of mean velocity is ~2 mm above the ground board in released fluid studies. Constructing a detailed aeroelastic model at that size is not practical. As well, the released fluid simulations only represent weak full-scale events.

2.2 Impinging jet experiments

Higher intensity flows are simulated using blowing equipment as shown in Figure 6. Instead of releasing fluid from a container, a mounted nozzle directs an air jet towards a ground board. A wall jet that bears similarities to the microburst outflow is created in the test section. Holmes [9] discusses the development of this approach and extensive literature reviews have been carried out on this topic [10, 11].

The majority of impinging jet studies use a continuous flow, implicitly assuming that the peak gust in the microburst outflow can be modelled with a steady wall jet. At low heights, the mean velocity profiles from quasi-steady simulations show reasonable agreement to full-scale measurements [11, 12]. However, field measurements of turbulence intensities and Reynolds stresses are presently lacking, thus limiting the validation of this approach.

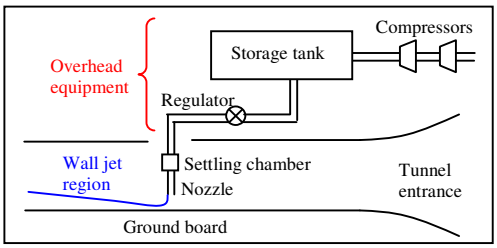

Figure 6: *Typical impinging jet apparatus.*

The key outflow characteristics, identified in Section 2, should be addressed. In this regard, the released flow studies have an advantage since they are inherently transient. Recent impinging jet studies find that the short duration of the intense outflow and the dominant vortex ring can be simulated by either:

(1) the initial flow from an impulsively started jet with steady boundary conditions [13], or
(2) a steady-state jet actuated at the nozzle with a gating device [14].

Impulsively started computational [13] and quasi-steady experimental [15] results show that the outflow region is not greatly affected by the nozzle height above the ground board. Computational results with the released fluid approach [6] also show insensitivity of the outflow to release height. This consistency favours the notion that the outflow region can be approximated as being independent of the downdraft region.

As with the released fluid set-up, the vertical size of the impinging jet outflow is limited due to overhead apparatus. As seen from Figure 6, blowing equipment occupies a large amount of the available space above the ground plane. As a result the vertical size of the test section wall jet is limited.

The impinging jet microburst simulations can be approximately one order of magnitude larger than the released fluid experiments. However, this is still too small to study wind loads on detailed models. Estimates of the scaling in previous studies are provided in Table 1.

Study	Geometric scale	Velocity scale	Comments
Buoyancy-driven flow			
Lundgren *et al* [6], experimental	1:22000 (1:9000 - 1:45000)	1:85	Release of fluid from a stationary cylinder vessel into a tank of ambient fluid of lesser density
Alahyari & Longmire [7], experimental	1:25000	1:300	
Impinging jet			
Kim *et al* [13], computational	1:26000 (1:10500 - 1:52500)	1:6.7	Impulsive start of a stationary continuous jet
Mason *et al* [14], experimental	1:3000 (1:2400 - 1:6100)	1:3	Actuated stationary continuous jet
Slot jet (present results with preliminary facility)			
Quasi-steady simulation	1:800 - 1:4000	-	2-D slot jet
Transient simulation	1:700	1:2	
Slot jet (anticipated results with full-size facility)			
Quasi-steady simulation	1:200 - 1:1000	-	2-D slot jet, 6.75 times larger than small facility
Transient simulation	1:700	1:1 - 1:2	

N.B. *Nominal values are quoted from the original papers, where given. The range in brackets is based on the definition of a microburst outflow being 0.4-2.0 km in radius. Note that velocity scaling for buoyancy-driven flow studies are based on weak full-scale events with maximum radial velocity of ~12 m/s, whereas the impinging jet and current studies scale to the strongest full-scale events with maximum radial velocity > 50 m/s.*

Table 1: *Scaling of previous and present transient flow simulations.*

3. PRESENT APPROACH

By neglecting the downdraft column, the outflow region can be simulated at a larger scale. This approach is analogous to that used for urban ABL simulation. For wind loading studies, it is sufficient to simulate just the lower third of the total ABL thickness (at 1:100 - 1:250 scale). Wind tunnel boundary layer spectra show good agreement with full-scale data using that approach [16]. Thus, a suitably large flow for model testing is achieved in a wind tunnel of economical size (typically of height = 1m and fetch ≈ 5 m).

Similarly, the present work focuses only on the microburst region that directly affects the urban environment. With this approach, the blowing equipment in Figure 6 above the ground board is not required. Without the overhead nozzle and other components, the vertical extent of the simulated outflow can be increased.

The present approach simulates a microburst outflow by expelling fluid from a rectangular slot. The present results are from a preliminary facility constructed to test the general concept. The same design will be scaled up to a larger facility (a modular addition to an existing large, open-return boundary layer wind tunnel).

Table 1 shows the estimated scale of the transient flow simulation in the preliminary facility and the full-size microburst outflow simulator, which is to be larger by a factor of 6.75. The full-size facility will simulate a significantly larger outflow in comparison with previous investigations. The test section velocities will also be close to full-scale.

The geometric scale of the preliminary facility transient simulation is found by comparing an experimental time history to recorded field data. An empirical model [17] is applied to find a best fit to the data from Figure 3. The characteristic velocity and time scales are then estimated based on the empirical model.

The rise to peak velocity (U_p), above the ambient value, is used as the characteristic full-scale velocity. Summing the durations for rise to peak and decay to half of peak velocity gives a characteristic time scale, $T_{0.5\ Up}$. These values are determined as shown in Figure 7.

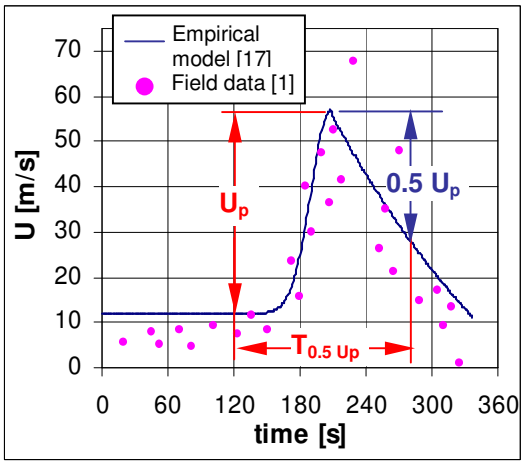

Figure 7: *Determining characteristic scales from a full-scale time history.*

The same quantities are found from an experimental time history. Characteristic length scale is taken as the product of the velocity and time scales. The scaling shown in Table 1 for the transient simulation in the preliminary facility is determined from Equation 1.

$$\frac{(U_p \cdot T_{0.5Up})_{\text{full-scale}}}{(U_p \cdot T_{0.5Up})_{\text{experimental}}} \qquad (1)$$

4. EXPERIMENTAL SET-UP

The transient nature of a microburst is modelled using a gate near the slot exit. As depicted in Figure 8, the gate is actuated using a stepper motor assembly. Connecting rods are rigidly fastened to the gate and a link bar, and thus, these components translate as a rigid assembly.

A *Delrin*® nut is also fixed to the link bar. The matching threaded rod is mounted concentrically on the stepper motor shaft. Thus, rotational motion of the motor shaft is changed into 13.5 mm of vertical travel, the distance required for the gate to fully open/close the slot.

The stepper motor allows simple and accurate control over the gate motion. One complete shaft revolution of the selected motor consists of 200 steps. The digital control allows precise incremental gate positioning without the complexity of implementing a feedback system. Since the shaft is aligned with exact pole positions electromagnetically, the gate motion is precise and repeatable with minimal mechanical wear. In the powered standstill condition, a large holding torque holds the gate firmly shut. With the selected threaded rod, the linear gate motion is controlled with a resolution of 0.13 mm.

At the start of the transient simulation, the gate is initially shut and the fan is in steady operation. When the gate is opened, the static pressure that has built up behind the gate converts to the dynamic pressure associated with U_j. By immediately shutting the gate after it opens fully, a good representation of the microburst time history is achieved.

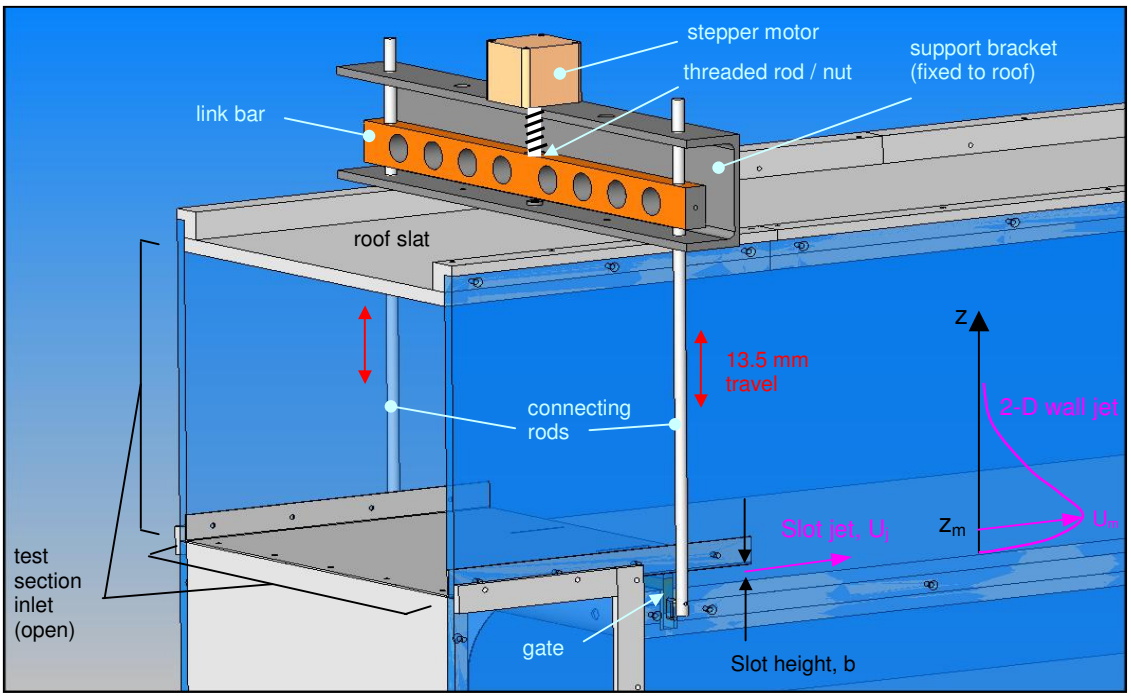

Figure 8: *A gate assembly to simulate the transient features of the microburst outflow.*

Downstream of the slot exit, the flow evolves into the characteristic wall jet profile as sketched in Figure 8. When the gate opens and shuts during each test run, a burst of air is emitted. With a sufficiently rapid gate actuation, the dominant vortex shown in Figure 9 is observed. The shutting phase of the gate motion is critical and a shutting duration of 0.18 s is maintained in the following results.

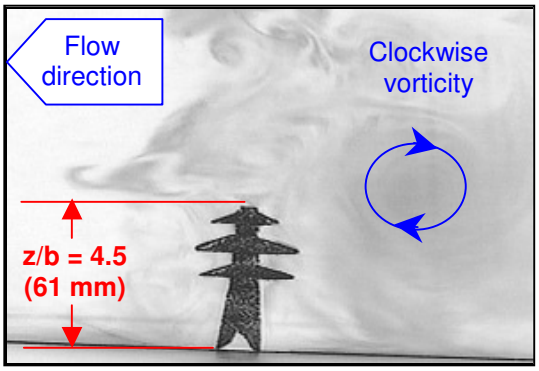

Figure 9: *Fog fluid visualization of the transient flow.*

4.1 Velocity measurement system

In the present work, mean velocities, turbulence intensities, and Reynolds stresses are of primary interest. Hot-wire anemometry (HWA) is a suitable measurement technique for transient flow measurements, because of its ability to discern high frequency components in a fluctuating signal. However, unless multiple probes are employed, HWA gives measurements at a single location only. Velocity profiles are built up from multiple runs wherein the probe is traversed incrementally in a plane of interest in the working section.

The cross-wire probe is positioned using a two-axis traverse. The traverse system is integrated with the gate and HWA systems, such that fully automated measurements over an entire plane can be done. The linear resolution of the probe positioning is significantly less than 1.0 mm, in both vertical and horizontal directions.

A Miniature Constant Temperature Anemometry system from Dantec Dynamics is used with a 55P61 cross-wire probe. Two velocity components are measured simultaneously. The maximum frequency response of the system is 10 kHz.

4.2 Experimental methodology

The transient jet tests require brief measurements at numerous locations. Composite vertical profiles are built up from ten realizations at each location to avoid the cost and risk involved with using a rake of hot-wire probes. The ten realizations at each location are sorted to reject poorly executed actuations (e.g. a clear lag of the peak due to a slow gate closing phase). The remaining actuations taken at a location are averaged.

This procedure gives an ensemble average time history for each spatial location. From the time histories, spatial profiles at specified times are derived. Thus, the temporal evolution of the vertical profiles of ensemble averaged velocity is extracted.

5. Experimental Results

The transient simulation is most relevant at streamwise locations where the expelled vortex remains coherent. Flow visualization and initial HWA measurements indicate that the region of interest is at x/b < 50. Here, results are shown for three x/b locations, where b is the height of the slot opening (see Figure 8).

A check of the two-dimensionality of the transient flow is done at x/b = 30. Composite velocity profiles for vertical traverses at midspan and two other spanwise locations are compared in Figure 10. Each composite profile is associated with a reference time (t = elapsed time since the gate began to open).

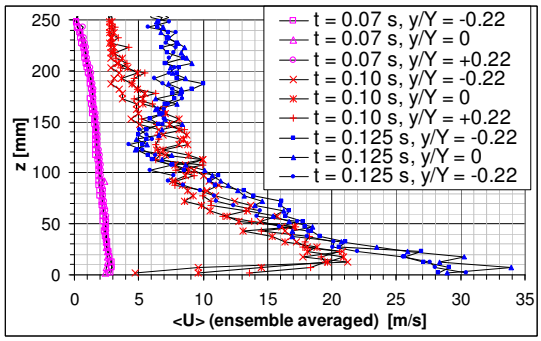

Figure 10: *Two-dimensionality of composite profiles at x/b = 30 for a transient wall jet over a smooth surface.*

The composite profiles at the three different times clearly show the temporal development of

the wall jet. The profiles at different spanwise locations and coincident reference times collapse reasonably well considering that the flow is unsteady. Also, note that the peak in the composite profile moves closer to the ground plane as its averaged velocity magnitude increases.

Figures 11 and 12 depict the temporal development at two other streamwise locations. The time of maximum peak velocity is indicated in the legend in red. Profiles with red markers build up to the maximum peak, and profiles with blue markers show the decay from the maximum peak. The maximum peak velocity is again close to the ground plane, and the height at which it occurs is fairly constant for the streamwise locations shown.

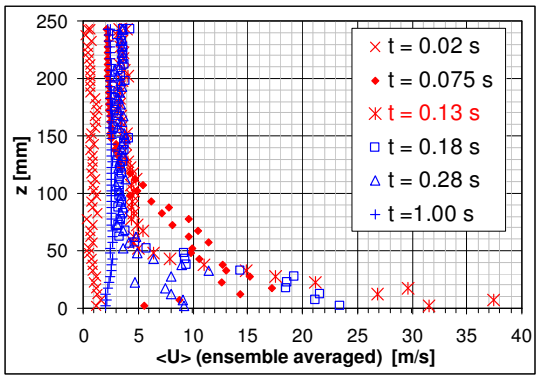

Figure 11: *Composite profiles at x/b = 20 and midspan for a transient wall jet over a smooth surface.*

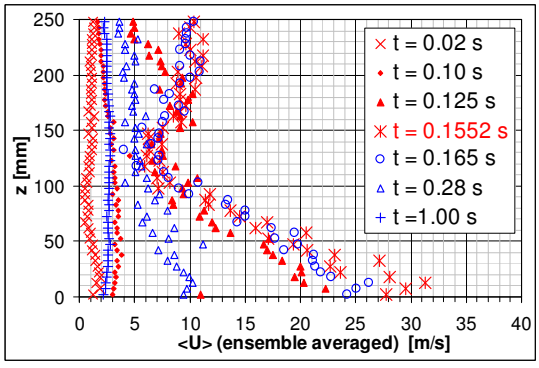

Figure 12: *Composite profiles at x/b = 40 and midspan for a transient wall jet over a smooth surface.*

Besides the low heights of the peak magnitude, the peak instantaneous value in a transient wall jet appears to have some speed-up, when compared to an equivalent steady jet. Fan speed is constant during the transient tests, and the transient effect is solely produced by the gate actuation. A speed-up of ~16% is found, which could perhaps be due to the dominant vortex ring. Note that the direction of the vorticity favours acceleration of the low-level flow. Further work will aim to clarify this issue.

6. DISCUSSION

A criticism of the actuated gate approach is that the duration of the gate actuation is not insignificant relative to the timescale of the developing transient flow. As found by other workers [14, 15], it is difficult to decrease the duration of gate actuation to less than the order of tenths of a second. Furthermore, the relation between duration of gate actuation and vortex characteristics is not presently clear.

If it is not possible to increase the speed of the gate actuation, such that complications such as shape effects are rendered negligible, it may be useful to characterize the transient simulation with a non-dimensional quantity. A transient burst released with a gate may be dependent upon:

(1) the open-gate, steady-state slot exit velocity equivalent to the static pressure that builds up when the gate is shut ($U_{j,ss}$), and

(2) the duration of the gate actuation (t_a).

The height of the maximum peak velocity ($z_{m,p}$) is a length scale of interest. Thus, $(U_{j,ss})\cdot t_a/(z_{m,p})$ may be a useful parameter in future work.

7. CONCLUSIONS OR SUMMARY

Improving the current understanding of extreme wind loads, such as those that arise from microbursts, will aid future structural design. Due to the difficulty of field experiments, laboratory simulations of microbursts are done. Previous studies using the released fluid and impinging jet methods have clarified the fluid mechanics of the microburst. The next step is to investigate the fluid-structure interaction, so that current design codes may be evaluated more knowledgably with regards to this preternatural event.

To facilitate wind tunnel testing of detailed structures, a microburst outflow simulator is designed. The primary innovation of the current

design is its capability to create large flows similar to microburst outflows. To advance beyond the basic quasi-steady approach, it is essential to simulate the transient features of the microburst outflow. The current novel design is capable of doing so, as verified with the preliminary facility results presented here. Work on a full-size facility, which can accommodate aeroelastic testing of transmission line tower models, is underway.

8. ACKNOWLEDGEMENTS

The Natural Sciences and Engineering Research Council of Canada, Manitoba Hydro, and the Institute of Catastrophic Loss Reduction provided the financial support for this work.

C. Vandelaar and B. Stuart from the UWO University Machine Shop provided input on the mechanical design and fabricated critical parts. Some equipment used in this research was kindly made available by G.A. Kopp and R.J. Martinuzzi. UWO technical staff and fellow research group colleagues provided assistance and support.

9. BIBLIOGRAPHY

[1] Fujita, T. T., The downburst: microburst and macroburst, Satellite and Mesometeorology Research Project, Research Paper #210; University of Chicago, Dept. of Geophysical Sciences, 1985.

[2] Hangan H., Savory E., Yu P., Surry D., Ho E., El Damatty A., Parke G., Disney P., Toy N. and White B., Modeling and prediction of failure of transmission lines due to high intensity winds, Phase 1 final report for Manitoba Hydro, Canada, January 2005.

[3] Holmes, J.D., Wind loading of structures, Spon Press, New York, NY, USA, 2001.

[4] Fujita T.T., Tornadoes and downbursts in the context of generalized planetary scales, Journal of Atmospheric Sciences, **38**(8):1511-1534, 1981.

[5] Alahyari A.A., Dynamics of laboratory simulated microbursts, University of Minnesota, PhD thesis, 166 pages, December 1995.

[6] Lundgren T.S., Yao J. and Mansour N.N., Microburst modelling and scaling, Journal of Fluid Mechanics, **239**:461-488, 1992.

[7] Alahyari A. and Longmire E.K., Dynamics of experimentally simulated microbursts, American Institute of Aeronautics and Astronautics Journal, **33**(11):2128-2136, 1995.

[8] Yao J. and Lundgren T.S., Experimental investigation of microbursts, Experiments in Fluids, **21**:17-25, 1996.

[9] Holmes J.D., Modelling of extreme thunderstorm winds for wind loading of structures and risk assessment, Wind Engineering into the 21st Century, Proceedings of the 10th International Conference on Wind Engineering, 21-25 June, Copenhagen, Balkema, Netherlands, 1409-1415, 1999.

[10] Letchford C.W., Mans C. and Chay M.T., Thunderstorms – their importance in Wind Engineering (a case for the next generation wind tunnel), Japan Association for Wind Engineering, Journal of Wind Engineering, **89**:31-43, October 2001.

[11] Lin W.E., Large-scale physical simulation of a microburst outflow using a slot jet, University of Western Ontario, MESc thesis, 229 pages, December 2005.

[12] Wood G.S., Kwok K.C.S., Motteram N.A. and Fletcher D.F., Physical and numerical modelling of thunderstorm downbursts, Journal of Wind Engineering and Industrial Aerodynamics, **89**:535-552, 2001.

[13] Kim J., Ho T.C.E. and Hangan H., Downburst induced dynamic responses of a tall building, 10th Americas Conference on Wind Engineering, Baton Rouge, Louisiana, 2005.

[14] Mason M.S., Letchford C.W. and James D.L., Pulsed wall jet simulation of a stationary thunderstorm downburst, Part A: Physical structure and flow field characterization, Journal of Wind Engineering and Industrial Aerodynamics, **93**:557-580, 2005.

[15] Xu Z., Experimental and analytical modeling of high intensity winds, University of Western Ontario, PhD thesis, 184 pages, December 2004.

[16] Cook N.J., On simulating the lower third of the urban adiabatic boudary layer in a wind tunnel, Atmospheric Environment, **7**:691-705, 1973.

[17] Holmes J.D. and Oliver S.E., An empirical model of a downburst, Engineering Structures, **22**:1167-1172, 2000.